Journal of Applied Electrochemistry **32**: 369–377, 2002.

Potential and concentration gradients in a hybrid ion-exchange/electrodialysis cell

P.B. SPOOR, L. KOENE* and L.J.J. JANSSEN
Eindhoven University of Technology, Department of Chemical Engineering, Laboratory of Process Development, PO Box 513, 5600 MB Eindhoven, The Netherlands
*(*author for correspondence, e-mail: L.Koene@tue.nl)*

Received 23 August 2001; accepted in revised form 29 January 2002

Key words: electrodeionization, electrodialysis, ion exchange, mathematical simulation, nickel

Abstract

The regeneration of 2, 4 and 8% cross-linked ion-exchange resins in the nickel-form was carried out in a three-compartment hybrid ion-exchange/electrodialysis cell. During the process the potential and nickel concentration profiles in the bed were measured. The experimental results are compared to results from a one-dimensional transport model able to simulate the development of potential and concentration gradients during the process; the amount of nickel transported out of the ion-exchange bed to the cathode, or concentrate, compartment was also reasonably well predicted. Differences between the model and experimental results are also discussed. It was found that under extreme conditions (i.e., high bed voltage), the formation of metallic nickel was observed in the central ion-exchange compartment.

List of symbols

A	area (m^2)
c_i	concentration of species i (mol m^{-3})
D_i	apparent diffusion coefficient of species i (m^2 s^{-1})
d	bed thickness (m)
ΔE_{bed}	potential drop across ion-exchange bed (V)
E, φ	potential in ion-exchange bed (V)
F	faradaic constant (C mol^{-1})
i	current density (A m^{-2})
N_i	flux of species i (mol m^{-2} s^{-1})
n_i	number of moles species i
R	universal gas constant (J mol^{-1} K^{-1}, VC mol^{-1} K^{-1})
T	temperature (K)
t	time (s)
X_i	fraction of ion i
x	position along axis
z	valence (−)
ω	charge of fixed sites within ion-exchange resin (−)

Subscripts

a	anode compartment
bed	bed of ion-exchange resin occupying centre compartment
c	centre compartment
fixed	fixed ionogenic sites in ion-exchange resin
k	cathode compartment
m	membrane

Superscripts

0	initial value at $t = 0$
descr	descriptive
max	maximum

Note: over-bars indicate values within resin

1. Introduction

A hybrid ion-exchange/electrodialysis system is being studied for the treatment of very dilute galvanic nickel waste solutions. The aim of the hybrid system is to increase the selectivity and conductivity of an electrodialysis-type cell by placing a bed of ion-exchange particles in its diluate compartment. The transport of ions out of the waste solution is enhanced when the increase in ionic concentration between the solution and resin phases is greater than the decrease in ionic mobility, this is because the ionic flux is directly proportional to both ionic concentration and mobility. A 1 mol m^{-3} Ni^{2+} solution, for example, can experience a 500-fold increase in concentration when sorbed by a resin with a Ni^{2+} capacity of 534 mol m^{-3} [1], while a 60-fold decrease in the apparent diffusivity can occur (7×10^{-10} m^2 s^{-1} in the solution phase [2] vs 1×10^{-11} m^2 s^{-1} in the resin phase [1]). This results in a considerable improvement in the removal rate, especially during

the treatment of solutions in the 'ppm' range. Also, in previous work [1, 3–5], as well as in work by others [6], no rate inhibition to mass transfer has been observed at the particle–particle, or particle–membrane surfaces. This provides another advantage of the hybrid system.

Several factors regarding the removal of sorbed divalent metal ions from a bed of ion-exchange particles using an applied electrical potential have been reported in previous papers [1, 3–5], and a description of pilot scale experiments carried out at a galvanic plant is given in [7]. This paper focuses on the concentration and potential gradients that develop in the cell during the regeneration of an ion-exchange bed initially in the nickel form. The results are compared to a simple transport model based on the Nernst–Planck equation. This approach has already been used to study similar systems, such as the removal of Cu^{2+} from solution using the 8% cross-linked Dowex HCR-S ion-exchange resin [8]. It has been found [1, 3–5], however, that high cross-linked resins are less suitable for use in the hybrid ion-exchange/electrodialysis cell since the diffusion coefficients of divalent ions within them are relatively low; compare, for example, the apparent diffusion coefficient of Cu^{2+} in the HCR-S resin (i.e., 4.3×10^{-12} m^2 s^{-1} [8]) to that of Ni^{2+} in the Dowex 50WX-2 (2% cross-linked) resin (i.e., 1.1×10^{-11} m^2 s^{-1} [4]). It is expected that the accuracy of this model will decrease as the degree of cross linking is reduced. This is primarily due to the increased ability of lower cross-linked resins to swell [9], and for this reason Dowex 50WX resins with 2, 4 and 8% cross-linking were studied. The resin with 8% cross linking can be considered as rigid. It should be noted that these swelling affects play a minor role during actual operation of the electrodialysis cell (i.e., simultaneous regeneration of the bed and sorption of ions from a feed solution) since the bed will be kept in a steady state where the rate at which ions are removed from the bed will equal the rate at which ions are sorbed from solution.

2. Theory

The model presented in this paper involves the Nernst–Planck equation (Equation 1). This equation has been used to model various ion-exchange processes such as ion-exchange [9, 10], electromigration in ion-exchange particles [9] and membranes [9, 11–13] as well as the hybrid system [8, 14, 15] and other similar systems [16].

$$N_i = -\bar{D}_i\left(\frac{\partial \bar{c}_i}{\partial x} + z_i \bar{c}_i \frac{F}{RT}\frac{\partial \varphi}{\partial x}\right) \tag{1}$$

The model requires the electric charge of the ionic species (z_i), diffusion coefficients ($\bar{D}_i$), bed voltage drop ($\Delta E = E_d - E_0$), bed width (d), initial nickel concentration in the bed ($\bar{c}^0_{Ni}$), concentration of fixed sites ($\bar{c}_{fixed}$), and the charge of fixed sites (ω) as input. This approach differs from that described in [8] as it models a system at constant bed voltage drop as opposed to constant current. Since changes in the interstitial solution conductivity may occur during actual application of the system to industrial waste treatment, this approach is taken to ensure a constant flux of ions within the ion-exchange particles. It considers the ion-exchange bed as a porous, macroscopically homogeneous system where the inputs mentioned above refer to the volume, cross section and length of the ion-exchange bed. They can, therefore, be obtained by macroscopic measurements. The model assumes no convection, constant diffusion coefficients, constant particle contact-area, and a constant concentration of fixed ionogenic groups. Moreover, the model assumes a uniform distribution of counter ions in the pores. A graphical representation of the model parameters is depicted in Figure 1.

The potential and concentration profiles as a function of place and time, the fluxes of H^+ and Ni^{2+} and the current as a function of time, as well as the amount of nickel removed from the bed can be calculated using the model.

The diffusion coefficient, $\bar{D}_i$, is an effective constant and as such incorporates all interactions of the counter ion within the resin; that is, counter ion–counter ion, counter ion–water, counter ion–fixed group, counter ion–matrix. By using this effective parameter the model does not take swelling effects into account. The swelling of the particles can affect the concentration of fixed sites, the diffusion coefficients and the contact area of the particles.

Along with Equation 1, the following factors were incorporated into the model:

(a) Sum of the fluxes

$$i = F\sum_i z_i N_i \tag{2}$$

with $i = 1, 2$ where $1 = Ni^{2+}$ and $2 = H^+$.

(b) Electroneutrality

$$\sum_i z_i \bar{c}_i = -\omega \bar{c}_{fixed} \tag{3}$$

where ω is the sign of fixed charges and $\bar{c}_{fixed}$ the concentration of fixed charges in the bed. In this case, Equation 3 takes the form

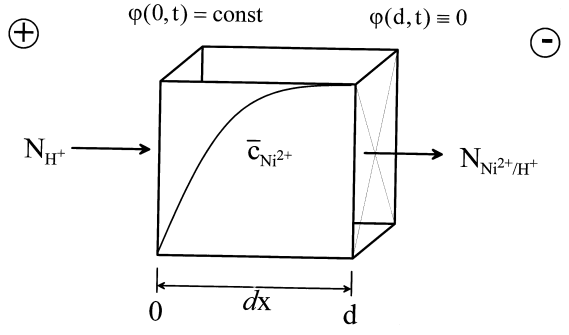

Fig. 1. Scheme of process.

$$2\bar{c}_{\mathrm{Ni}}(x) + \bar{c}_{\mathrm{H}}(x) = \bar{c}_{\mathrm{fixed}} \tag{4}$$

(c) Mass balance

$$\frac{\mathrm{d}\bar{c}_i}{\mathrm{d}t} = -\frac{\mathrm{d}N_i}{\mathrm{d}x} \tag{5}$$

The boundary and initial conditions are given below. At the start of the process the bed was uniformly loaded with ions, the concentration gradient was therefore zero. Thus,

$$\frac{\mathrm{d}\bar{c}_i(x,0)}{\mathrm{d}x} = 0 \tag{6}$$

and the potential gradient was initially linear, that is,

$$\frac{\partial\varphi(x,0)}{\partial x} = \text{const.} = \frac{E_d - E_0}{d} \tag{7}$$

The potential at $x = d$ was defined to be zero. Thus,

$$\varphi(d,t) \equiv 0 \tag{8}$$

For the entire experiment, the current at $x = 0$ was defined as being solely due to the transport of hydrogen-ions, that is,

$$i_{\mathrm{H}}(0,t) = i(t) \tag{9}$$

while the total amount of nickel removed from the bed was calculated according to

$$n_{\mathrm{Ni}}(t) = \int_0^t N_{\mathrm{Ni}}(d,t)\mathrm{d}t \tag{10}$$

From the model it should follow that at $t = \infty$, the nickel concentration in the bed is zero for all x. Thus,

$$\bar{c}_{\mathrm{Ni}}(x,\infty) = 0 \tag{11}$$

In other words, the bed is in the H-form, that is,

$$\bar{c}_{\mathrm{H}}(x,\infty) = X \tag{12}$$

and that the current due to nickel is zero, that is,

$$i_{\mathrm{Ni}}(x,\infty) = 0 \tag{13}$$

3. Experimental details

An experimental set-up similar to that described in [3] was used. It consisted of a three-compartment cell connected to separate liquid circuits (Figure 2). The outer anode and cathode compartment circuits each contained a 1 M H_2SO_4 electrolyte while the centre compartment was filled with Dowex 50W ion-exchange resins in the nickel form. The compartments were separated by two Nafion® 117 cation selective membranes; each had an effective area of 0.0010 m^2. The outer compartments had dimensions of 0.01 m × 0.1 m × 0.005 m and each contained a platinum plate electrode with dimensions of 0.01 m × 0.1 m. A centre compartment with a relatively large width was used to study the concentration and electrical potential gradients that developed during the process. This had dimensions of 0.01 m × 0.1 m × 0.1 m.

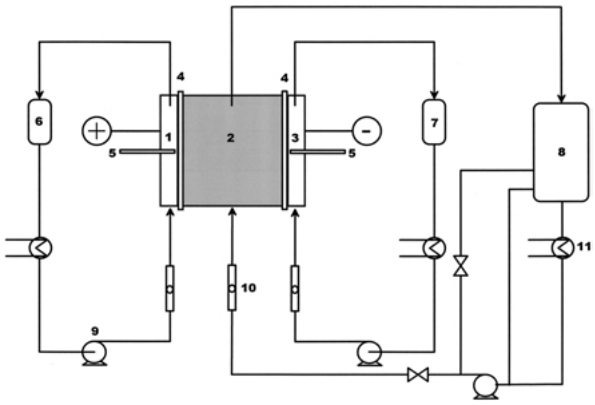

Fig. 2. Experimental set-up (cell enlarged for clarity). (1) Anode compartment, (2) ion-exchange bed, (3) cathode compartment, (4) cation-selective membranes, (5) Luggin capillaries, (6) anolyte reservoir, (7) catholyte reservoir, (8) rinse solution reservoir, (9) pump, (10) flow meter, and (11) heat exchanger.

To measure the electrical potential in the centre compartment, four silver wire electrodes were placed equidistant into the side of the compartment at a height of 0.05 m. The concentration gradient in the ion-exchange bed was determined by removing small quantities of the bed from the top of the cell. A lid located at the top of the centre compartment held the bed in place during the process and allowed access to the bed when removed.

Experiments were carried out using fully nickel loaded Dowex resins with 2, 4 and 8% cross linking (these resins have H^+ capacities of 0.6, 1.1 and 1.7 meq cm^{-3}, respectively). The resins were loaded with nickel by placing them, originally in the hydrogen form, into a column and passing a 0.2 M $NiSO_4$ solution through the bed until the pH of the effluent was equal to the pH of the original nickel solution. They were then washed with deionized water and subsequently placed in the centre compartment of the cell. The centre compartment was fed from the bottom with deionized water at a flow rate of 33 cm^3 min^{-1} to prevent dehydration of the resin, while sulfuric acid solutions were circulated through the outer compartments. A bed voltage of 20 V was applied for resins with 2 and 4% cross linking while the 8% cross-linked resin was regenerated at 40 V; the higher voltage was used to reduce the time of the experiment (in previous work, the rate of regeneration was found to be directly proportional to the bed voltage [4]). Additional experiments were carried out with the 2% cross-linked resin at bed voltages of 40 and 50 V.

The electric potential difference was kept constant between two calomel reference electrodes connected to two Luggin capillaries placed about 2 mm from each

membrane. The system was kept at a constant temperature of 298 K and all experiments excepting that with the 2% cross-linked resin were run continuously. Due to the high degree of swelling and the high swelling pressures the 2% cross-linked resin produced upon regeneration [9], this experiment was run daily for 8 h so that proper operation of the cell could be ensured. Since the mobility of nickel decreases with increased cross linking, the duration of the experiments was varied. The 2, 4 and 8% cross-linked resins were regenerated for 24, 72 and 95 h, respectively. Various properties of the system were monitored during the experiments. The current was recorded continuously using a computer while catholyte and bed samples were obtained at different electrodialysis times.

Bed samples consisting of a small number of particles were obtained at 13 points along the bed. To obtain these samples electrodialysis and flow of all solutions were stopped for a period of about 15 min. The voltage distribution in the cell was obtained at various electrodialysis times using the silver electrodes: potential differences were measured with respect to the reference electrode located in the cathode compartment. Analyses of the catholyte and bed samples were carried out using flame atomic absorption spectroscopy (FAAS) and energy dispersive spectroscopy (EDS), respectively (Jeol Superprobe JXA-8600 SX measurements were made using an acceleration voltage of 20 kV and a beam current between 5 and 7 nA). Using EDS, the fraction of nickel in the resin samples was obtained by relating the atomic fraction of nickel in the resin with that of sulfur (since nickel has a valence of 2, it will coordinate with 2 sulfonic acid sites, SO_3^-, fixed on the resin); three or more particles from a sample were used to obtain an average nickel fraction. A detailed description of the FAAS procedure can be found in [3].

4. Results

During the regeneration of the bed by the application of a potential difference, a nickel/hydrogen front was observed to move across the bed towards the cathode compartment. The velocity of the front strongly depended on the degree of cross linking, so much so that after 24 h electrodialysis at a bed voltage of 40 V, the front had moved less than 1 cm through the 8% cross-linked resin. The 2% cross-linked bed, however, was nearly regenerated after 24 h electrodialysis at 20 V (Figures 3–5). These Figures represent concentration gradients determined at different electrodialysis times during the three experiments. The gradients began relatively sharp but increased in dispersion as electrodialysis continued. The overall percentages of regeneration of the 2 (Figure 3), 4 (Figure 4) and 8% (Figure 5) cross-linked resins were calculated using the concentration gradient measured at the end of the experiments, that is, by integration of X_{Ni} over x. They were found to be 86, 84 and 21%, respectively.

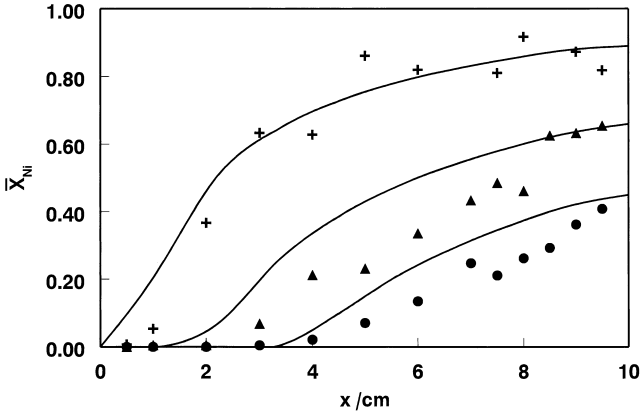

Fig. 3. Fraction of nickel in the 2% cross-linked resin as a function of distance, x, at $t = 8$ (+), 16 (▲) and 24 h (●); $\Delta E_{bed} = 20$ V. Model results are given as solid lines.

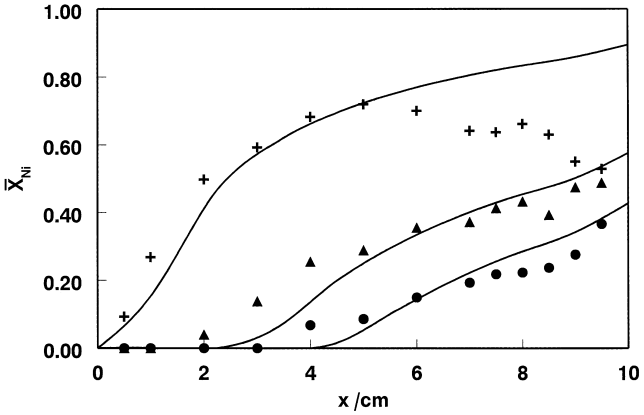

Fig. 4. Fraction of nickel in the 4% cross-linked resin as a function of distance, x, at $t = 24$ (+), 55 (▲) and 72 h (●); $\Delta E_{bed} = 20$ V. Model results are given as solid lines.

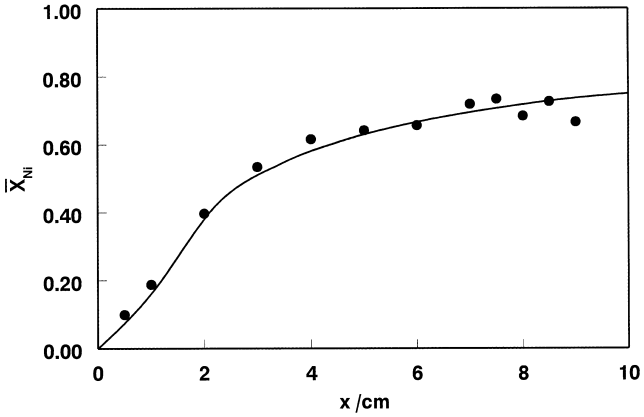

Fig. 5. Fraction of nickel in the 8% cross-linked resin as a function of distance, x, at $t = 95$ h; $\Delta E_{bed} = 40$ V. The model result is given as a solid line.

The potential distribution at various times of electrodialysis for the 2% experiment is shown in Figure 6. The potential distribution was originally linear for all experi-

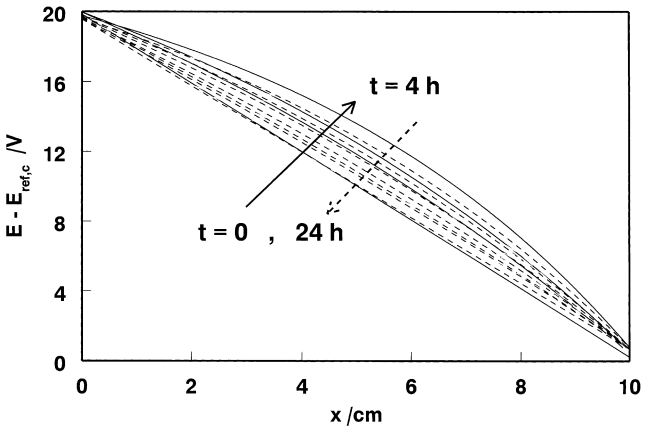

Fig. 6. Electric potential distribution as a function of distance, x, measured at various electrodialysis times for the 2% experiment at 20 V. The curvature of the distribution increases from $t = 0$ to 4 h (solid lines) and decreases from $t = 4$ to $t = 24$ h (dashed lines).

ments but as regeneration progressed, the distribution curved. This curvature arose as the potential gradient decreased in regenerated areas of the bed. During regeneration of the 8% cross-linked resin, the curvature of the distribution increased for the entire 95 h experiment. For the other two experiments however, the potential distribution reached a maximum curvature and subsequently returned to its original state; the 'maximum curvature' was reached after about 4 and 24 h for the 2 and 4% cross-linked resins, respectively.

Figure 7 clearly shows that the flux of nickel out of the bed decreased with increased cross linking. It also shows that the flux was not constant during electrodialysis but, for cross linking of 2 and 4%, had a maximum at t about 4 and 24 h, respectively (inflections in Figure 7). The various capacities of the three types of resin account for the differing magnitudes of nickel removed from the beds.

The results presented in Figures 3–5 and in Figure 7 were compared to the model described above; the outcome of the simulations are represented as solid lines in the figures. The parameters used for the calculations were obtained from various sources including previous work, literature and the experiments themselves. The apparent diffusion coefficients, $\bar{D}_{Ni}$, were estimated using the migration term of Equation 1 and an average nickel flux, N_{Ni}, determined by the slope of linear fit of the $n_{Ni,k}$ against t curves in Figure 7. The values used in the simulations were 4.87, 1.69 and 0.24×10^{-11} m^2 s^{-1} for the 2, 4 and 8% cross-linked resins, respectively.

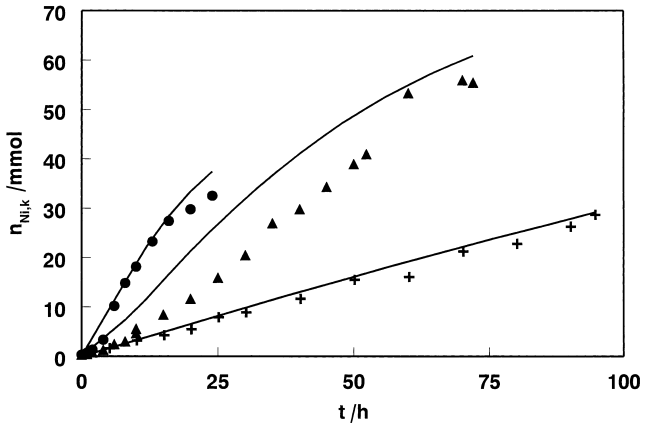

Fig. 7. Quantity of nickel in the catholyte versus electrodialysis time for the 2 (●), 4 (▲) and 8% (+) experiments. Model results are given as solid lines.

The initial concentration of nickel in the resin was experimentally determined for the 2 and 4% resins, they were found to be 534 [1] and 739 mol m^{-3}, respectively. Since the 8% cross-linked resin did not swell significantly, the capacity of the resin given by the supplier could be used to calculate the initial nickel concentration (i.e., 1700 mol m^{-3} H^+/2 eq Ni^{2+} = 850 mol m^{-3}). The model parameters are summarized in Table 1.

Evidently, the diffusion coefficients are functions of the nickel concentration of the resin (for a general description of this phenomenon, see Helfferich [9]). However, a 'descriptive' nickel diffusion coefficient was used to account for the dependence of $\bar{D}_{Ni}$ on $\bar{c}_{Ni}$. The descriptive diffusion coefficients for each experiment are given in Table 1; these do not have a rigorous physical meaning.

It was assumed that the diffusion coefficient of hydrogen in the bed, $\bar{D}_H$, is 10 times greater than that of nickel. This assumption is corroborated by literature results for the H^+ and Zn^{2+} forms of the older Dowex-50 resin [17], as well as unpublished current–voltage measurements performed on the hydrogen and nickel forms of the 2% cross-linked bed. The sensitivity of the diffusion coefficients on the model results will be examined later in this paper.

Figure 8 shows both experimental and model results for $n_{Ni,k}/t$ of the 2% ion-exchange resin. The Figure shows simulations using (a) the initial nickel diffusion coefficient, $\bar{D}^0_{Ni} = 1.33 \times 10^{-11}$ m^2 s^{-1} (this agrees well with previous work in which a value of $\bar{D}^0_{Ni} = 1.13 \times 10^{-11}$ m^2 s^{-1} was found by the same method [4]), (b) the maximum nickel diffusion coefficient during the 2% experiment $\bar{D}^{max}_{Ni} = 7.93 \times 10^{-11}$ m^2 s^{-1} (calculated from the nickel flux just before the inflection in the experimental curve given in Figure 7, at $t = 5$ h, as well as the potential gradient and nickel concentration in the cathode side of the bed at this time), and (c) the descriptive diffusion coefficient $\bar{D}^{descr}_{Ni} = 4.87 \times 10^{-11}$

Table 1. Model parameters

Cross-linking	ΔE_{bed} /V m^{-1}	$\bar{c}^0_{Ni}$ /mol m^{-3}	$\bar{c}_{fixed}$ /mol m^{-3}	$\bar{D}^{descr}_{Ni}$ /10^{-11} m^2 s^{-1}	$\bar{D}^{descr}_{H}$ /10^{-10} m^2 s^{-1}
2%	200	534	1068	4.87	4.87
4%	200	739	1478	1.69	1.69
8%	400	850	1700	0.24	0.24

$z_H = 1$, $z_{Ni} = 2$, $d = 0.1$ m, $A_m = 0.001$ m^2, $\omega = -1$.

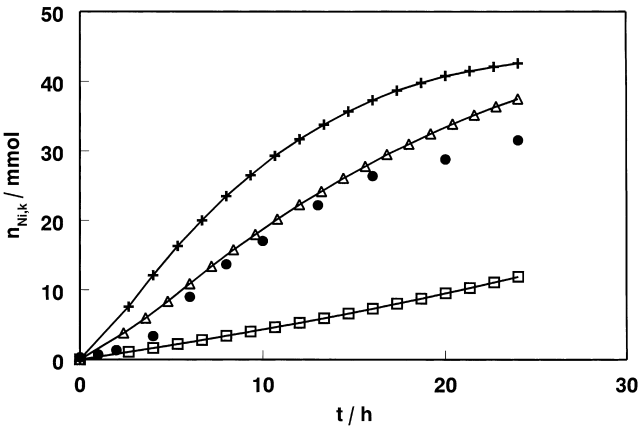

Fig. 8. Quantity of nickel in the catholyte versus electrodialysis time for the 2% experiment (●) along with simulations using $\bar{D}_{Ni} = 1.33 \times 10^{-11}$ (□), 4.87×10^{-11} (△) and 7.93×10^{-11} m^2 s^{-1} (+), respectively.

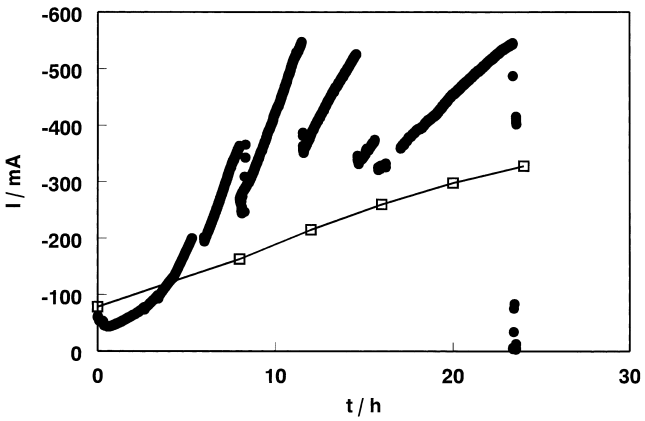

Fig. 9. Current as a function of electrodialysis time for the 2% experiment run at a bed voltage of 20 V (●). The sharp decreases at $t = 8.0$, 11.5, 14.5 and 16.0 h are due to the release of swelling pressure within the ion-exchange bed. Computer simulation is also presented (□).

m^2 s^{-1}. It is clear that the model calculation using the initial and maximum nickel diffusion coefficients lie well above and below the experimental result, respectively. The simulation using the descriptive nickel diffusion coefficient lies between and agrees reasonably with the experimental results.

Strong swelling effects were also observed during the 2 and 4% experiments. In previous work [1], the 2% cross-linked resin was observed to increase in volume by approximately 40% upon conversion from the nickel to the hydrogen form. Swelling causes an increase in the swelling pressure within the cell during the regeneration process, the greatest of which was observed during the 2% experiment and, to a lesser degree, the 4% experiment (approximately 20%). No swelling was observed during the experiment with the 8% cross-linked resin. The observed expansion of the bed out of the cell when its compartment was opened was one consequence of swelling. This portion was removed before bed samples were taken; this resulted in a decrease in swelling pressure within the bed when the process was restarted. Such changes in swelling pressure within the cell manifested itself mainly as fluctuations in current; Figure 9 depicts the current as a function of time for the experiment with a 2% cross-linked resin. During this experiment bed samples were taken every 8 h, while at $t = 11.5$ and 14.5 h excess resin was removed; a corresponding decrease in current is clearly observed at these times. The magnitude of the current decreases at $t = 8$, 11.5 and 14.5 h were 111, 194 and 190 mA, respectively; at 20 V these changes correspond to changes in bed resistance of 24, 20 and 22 Ω. The I/t result of the simulation is also given in Figure 9; the simulation calculated a current that roughly follows the minima of the current oscillations.

Three experiments were initially performed at a bed voltage of 50 V using the 2% cross-linked resin. About 1.5 to 2 h into these experiments the formation of a dark green layer in the bed on the cathode side membrane was observed. After about 4 h of electrodialysis the green layer had grown uniformly along the membrane to a about 2.5 mm into the bed. Samples taken from the bed showed that the green layer consisted of a precipitate attached to the outside of the ion-exchange particles. Small black particles, which grew with time, were subsequently observed in this region. After about 5–7 h electrodialysis time, the growth of the black particles was accompanied by the evolution of gas from the same region of the bed. One of the trials was allowed to run until the entire bed was regenerated. During this experiment, the potential distribution was measured periodically at 14 points along the top of the bed; the distribution at 6 and 12 h is given in Figure 10. After 6 h of experiment the dark green strip of precipitate was observed to reach a width of about 5 mm, the potential drop over this region was significantly high at 2800 V m^{-1} compared to 300 V m^{-1} over the remainder of the bed. At $t = 12$ h the potential drop over this region was considerably lower but the rate of gas

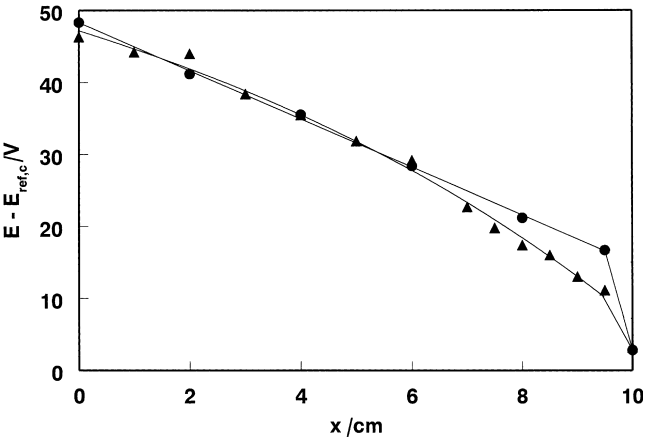

Fig. 10. Electric potential as a function of distance, x, for the 2% experiment run with a bed voltage of 50 V. The measurements were taken at $t = 6$ (●) and 12 h (▲). At $t = 6$ h, a 0.5 cm band of precipitate along with a small quantity of gas evolution was observed along the cathode side membrane. At $t = 12$ h the rate of gas evolution had increased dramatically.

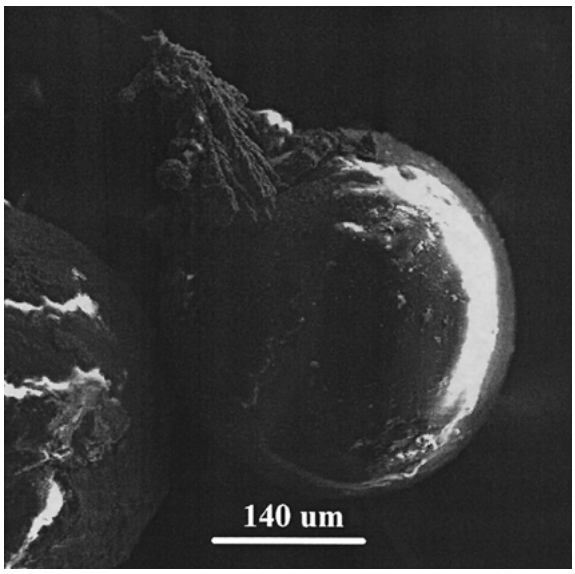

Fig. 11. Metallic nickel deposition protruding from an ion-exchange particle removed from the cathode side of the cell after the 2%/50 V experiment was completed; 180× magnification.

evolution had radically increased; the current at this time was 2.14 A compared to 0.97 A at $t = 6$ h.

Once regeneration of the bed was complete, the green strip of precipitate gradually disappeared leaving only the regenerated resin and the black particles. Upon removal of the ion-exchange bed, the black particles were separated using a magnet and EDS analysis showed that they consisted solely of nickel. Figures 11 and 12 show the metallic nickel attached to an ion-exchange particle at different magnifications; the dendritic structure of the deposit is clear at higher magnification. An additional experiment run at a bed voltage of 40 V also exhibited this behaviour.

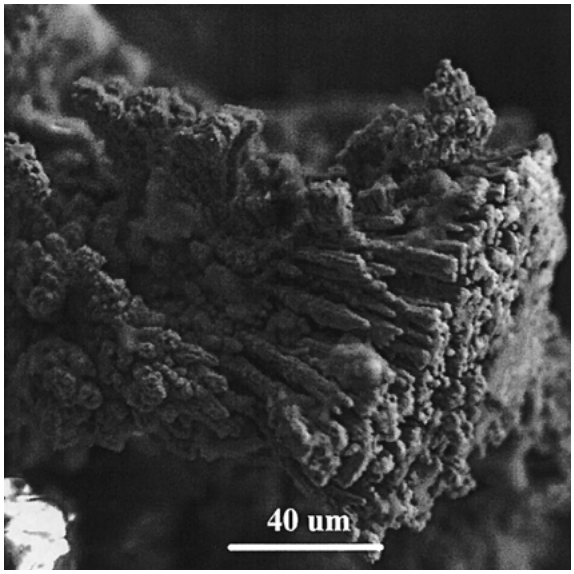

Fig. 12. Dendritic metallic nickel deposition found on an ion-exchange particle removed from the cathode side of the cell after the 2%/50 V experiment was completed; 650× magnification.

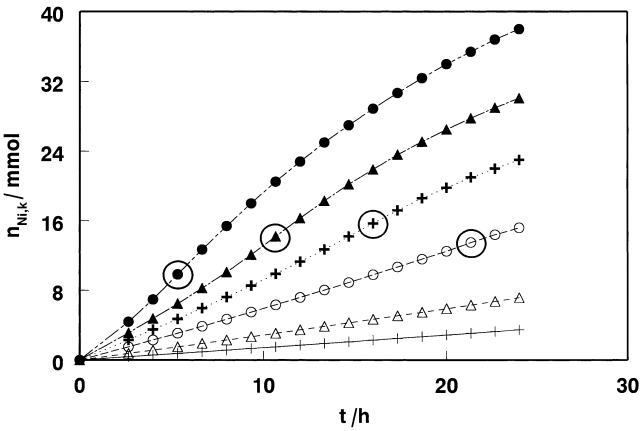

Fig. 13. Computer simulations at various degrees of nickel loading: 50 (+), 100 (△), 200 (○), 300 (+), 400 (▲) and 534 (●) mol m^{-3} out of a total set capacity of 534 mol m^{-3}. $\bar{D}_{Ni}$ and ΔE_{bed} were set at 5.0×10^{-11} m^2 s^{-1} and 200 V m^{-1}, respectively.

5. Discussion

Before discussing the relationship between the calculated and experimental results, it is worthwhile mentioning how the model behaves when the fraction of nickel in the bed is decreased and the $\bar{D}_H/\bar{D}_{Ni}$ ratio increased. Figure 13 shows simulated $n_{Ni,k}/t$ results of the former with $\bar{D}_{Ni} = 5.0 \times 10^{-11}$ m^2 s^{-1}, a maximum $\bar{c}_{Ni} = 534$ mol m^{-3}, and an electrodialysis time of 24 h (these parameters are similar to those of the 2% experiment). An increase in nickel flux with increasing nickel concentration is clearly observed, and there are obvious inflections in the curves at higher $\bar{c}_{Ni}$. The presence of these inflections can be understood by examining the simulated concentration and potential profiles within the bed. The circled points in Figure 13 represent the electrodialysis time at which $\bar{c}_{Ni}$ decreased (and $\bar{c}_H$ increased) at the cathode side of the bed, and these points also correspond to the time of 'maximum curvature' of the potential profile. It is also interesting to note that they fall on the inflection of the n_{Ni}/t curve. The reason for this behaviour arises from the difference between the hydrogen and nickel diffusion coefficients. When the nickel in the bed is replaced by the more mobile hydrogen ion, the resistance, and therefore the potential gradient, over the regenerated part of the bed will decrease. The potential gradient over the remainder of the bed, since the process is run at constant bed voltage, will increase. The increase in the potential gradient over the nickel-loaded portion of the bed will cause an increase in the flux of nickel out of the bed; this is represented by the n_{Ni}/t curves before the inflection. Once the fraction of hydrogen ions increases throughout the entire bed (i.e., the breakthrough of H^+ transport to the catholyte during the experiment with $\bar{c}_{Ni} = 534$ mol m^{-3}) the resistance of the bed and therefore the potential gradient over the bed will become increasingly uniform. The potential profile will then return to its original state and the flux of nickel out of the bed will decrease; this is represented by the n_{Ni}/t curve after the

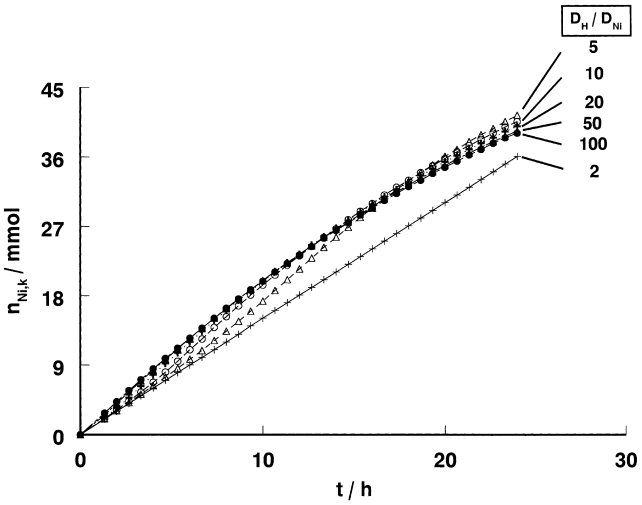

Fig. 14. Computer simulations at various $\bar{D}_H/\bar{D}_{Ni}$ ratios: 2 (+), 5 (△), 10 (○), 20 (+), 50 (▲) and 100 (●). $\bar{D}_{Ni}$ and ΔE_{bed} were 5.0×10^{-11} m^2 s^{-1} and 200 V m^{-1}, respectively, while $\bar{D}_H$ was varied.

inflection. Since the transport rate of Ni^{2+} increases with its concentration in the resin [3], the inflection in the n_{Ni}/t curve during the $\bar{c}_{Ni} = 50$ and 100 mol m^{-3} simulations occurs at later times and is not observed within the time frame of the simulation.

Since the difference between the H^+ and Ni^{2+} diffusion coefficients have been shown to influence the electrodialytic regeneration of the ion-exchange bed, simulations were also performed with a constant $\bar{D}_{Ni}$ (5.0×10^{-11} m^2 s^{-1}) and varying $\bar{D}_H$. The nickel concentration for all simulations was initially 534 mol m^{-3} (this concentration represents a nickel fraction in the bed of 1, or fully loaded). Figure 14 shows that for $\bar{D}_H/\bar{D}_{Ni}$ ratios between 2 and 100, the nickel flux increases with increasing $\bar{D}_H$ before the inflection while the opposite holds true after the inflection. This can be understood by again considering the relative decrease in the resistance of the regenerated portion of the bed at various $\bar{D}_H/\bar{D}_{Ni}$ ratios. The potential gradient over the regenerated portion of the bed will decrease by a degree dictated by the $\bar{D}_H/\bar{D}_{Ni}$ ratio (i.e., the larger the ratio, the larger the decrease), this means that the increase in the potential gradient over the remainder of the bed will also be dictated by this ratio. In other words, the 'maximum curvature' of the potential distribution over the bed will increase with increase in the $\bar{D}_H/\bar{D}_{Ni}$ ratio. Before the inflection, the flux of nickel out of the bed will therefore increase with increase in this ratio. Once the transport of H^+ has broken through to the catholyte, the flux of nickel out of the bed will be dictated by both the $\bar{D}_H/\bar{D}_{Ni}$ ratio as well as the nickel concentration in the resin at the cathode side of the bed.

Similar behaviour to that described above was found experimentally and as such, the simulations agreed reasonably well with the experimental results. The fit of the 8% experiment was most accurate as its degree of swelling was very small. Calculations for the 2 and 4% experiments, whose volumes in the nickel and hydrogen forms vary by approximately 40 and 20%, respectively, were less accurate.

As described above, the model was able to show a correlation between the time at which the flux of nickel to the catholyte began to decrease, the time at which a breakthrough of hydrogen at the cathode side was observed and the time at which the 'maximum curvature' of the potential distribution over the bed was reached. These correlations were also observed experimentally. The electrodialysis time at which the inflection of the $n_{Ni,k}/t$ curves occurred was predicted by the model for the 2 and 4% experiments (the 8% experiment showed no breakthrough of H^+ to the catholyte and hence no inflection). The *magnitude* of the 'maximum curvature' of the potential distribution as well as the slope of the n_{Ni}/t curves at the inflection, however, were not adequately predicted by the model. Figure 15 depicts the calculated potential distribution for the 2% experiment at various times, the change in the distribution was smaller than that obtained experimentally. The slope of the experimental curves at the inflection in Figure 7 are also much greater than that predicted by the model. These two factors are likely linked.

The strong swelling effects exhibited by the 2 and 4% cross-linked resins revealed themselves as a physical swelling of the particles out of the cell after it was opened, and as fluctuations in current (Figure 9). The conductivity of the ion-exchange bed increased due to the exchange of nickel ions with highly mobile hydrogen ions but it has also been shown that the 2% cross-linked bed decreased in resistance by as much as 24 Ω due to swelling pressure. The swelling pressure likely affected the contact area between the gel particles. When the pressure was released during the sampling process (which required the opening of the cell and the removal of excess resin), the conductivity of the bed dropped. The mathematical model, which did not account for changes in swelling pressure, reasonably predicted the

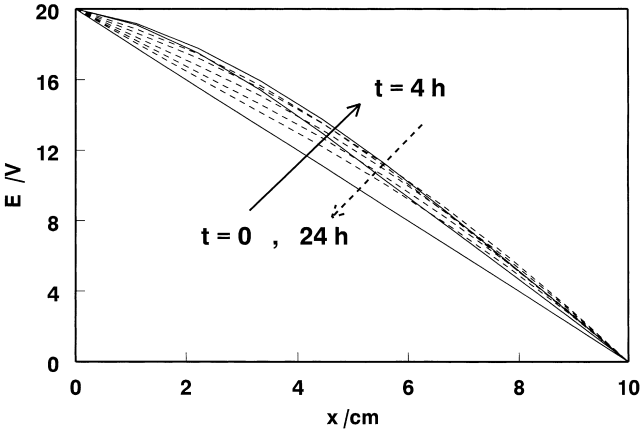

Fig. 15. Calculated electric potential distribution as a function of distance, x, at various electrodialysis times for the 2% cross-linked ion-exchange resin. The curvature of the distribution increases from $t = 0$ to 4 h (solid lines) and decreases from $t = 4$ to $t = 24$ h (dashed lines). The time of maximum curvature is about equal to that of the experimental results in Figure 6.

current immediately after the release of pressure within the cell (or at the minima of its oscillations).

The formation of metallic nickel was observed within the 2% cross-linked ion-exchange bed at high cell voltage. The electrochemical reduction of nickel ions in the cathode side of the bed was preceded by the formation of a layer of nickel hydroxide precipitate at the cathode membrane and was accompanied by gas evolution in the same region. The precipitation of nickel hydroxide was also observed in previous work [1], however, the latter process involved Ni^{2+} originating from solution and not from the ion-exchange particles. After the precipitate had begun to form, the potential difference over the region of the bed containing the precipitate increased and nickel reduction followed. Figure 10 clearly shows that the potential drop across the region in which metallic nickel was formed was large enough to facilitate its reduction. Once the bed had been fully regenerated to the hydrogen form, the nickel hydroxide precipitate was resorbed and transported to the cathode compartment. The dissolution of the precipitate, normally insoluble at higher pH [1], was possible due to the high acidity of the resin. The formation of nickel hydroxide, as well as metallic nickel, was not observed during the experiment with a bed of 8% cross-linked resin; the mobility of the nickel ions within the resin therefore plays a role in the process.

6. Conclusions

A model based on the Nernst–Planck equation offers a relatively simple method to describe the regeneration of a packed bed of ion-exchange particles using a constant applied potential difference as driving force.

Calculations using this model agreed reasonably well with experimental results, especially for a resin with a relatively high degree of cross-linking (i.e., the rigid 8%). The inability of the model to account for particle swelling meant that its accuracy decreased for resins of lower cross-linking, mainly because it changes the ionic diffusivities within the matrix of the resin. To account for these changes in diffusivity, the effect of the ionic concentrations upon the resin as well as the change in the contact area between the particles on the diffusivities should be taken into account. The experimental as well as the calculated results showed how the regeneration rate was affected by the changing electric potential distribution over the bed, which was in turn was affected by the changing distribution of ions within the bed. The resulting regeneration rate exhibited a maximum some time after the start of the experiments, a phenomenon not seen during similar experiments at constant current [8].

Experiments with resins of low cross-linking (i.e., the flexible 2%) also exhibited nickel precipitation and reduction within the 10 cm wide ion-exchange bed at high cell voltage.

Acknowledgements

We thank Ing. N.J.H.G.M. Lousberg for his assistance with the EDS analyses, Dr Ir. J.K.M. Jansen for his suggestions on the numerical mathematics and Q.D. Nguyen for his programming skills. We would also like to thank Senter for their financial support and TNO-MEP for their collaboration during this project.

References

1. P.B. Spoor, L. Koene, W.R. ter Veen and L.J.J. Janssen, *J. App. Electrochem* **32** (2002) 1–10.
2. R. Parsons, '*Handbook of Electrochemical Constants*' (Butterworths Scientific, London, 1969).
3. P.B. Spoor, W.R. ter Veen and L.J.J. Janssen, *J. App. Electrochem.* **31** (2001) 523–530.
4. P.B. Spoor, W.R. ter Veen and L.J.J. Janssen, *J. App. Electrochem.* **31** (2001) 1071–1077.
5. P.B. Spoor, L. Koene, W.R. ter Veen and L.J.J. Janssen, *Chem. Eng. J.* **85**(2–3) (2002) 127–135.
6. E. Korngold, *Desalination* **16** (1975) S225–S233.
7. P.B. Spoor, L. Grabovska, L. Koene, L.J.J. Janssen and W.R. ter Veen, *Chem. Eng. J.* accepted for publication.
8. J. Johann, Elektrodialytische Regenerierung von Ionenaustauscherharzen, PhD thesis (University of Stuttgart, 1992).
9. F. Helfferich, '*Ion Exchange*' (Dover, New York, 1995).
10. J.C.R. Turner, M.R. Church, A.S.W. Johnson and C.B. Snowdon, *Chem. Eng. Sci.* **21** (1966) 317–325.
11. P.N. Pintauro, A.G. Guzman-Garcia, M.W. Verbrugge and R.F. Hill, *AIChE J.* **36** (1990) 1061.
12. E.H. Cwirko and R.G. Carbonell, *J. Colloid Interface Sci.* **129** (1989) 513.
13. W.H. Koh and H.P. Silverman, *J. Membrane Sci.* **13** (1983) 279–290.
14. H.M. Verbeek, L. Fürst and H. Neumeister, *Comput. Chem. Eng.* **22** (1998) S913.
15. E. Dejean, J. Sandeaux, R. Sandeaux and C. Gavach, *Sep. Sci. Technol.* **33** (1998) 801–818.
16. I.W. Cumming, H. Tai and M. Beier, *Trans. IChemE.* **75** (1997) 9.
17. K.S. Spiegler and C.D. Coryell, *J. Phys. Chem.* **56** (1952) 106.